

Splitting Numerical Technique with Application to the High Resolution Simulation of the Indian Ocean Circulation

G.I. MARCHUK,¹ A.S. RUSAKOV, V.B. ZALESNY,¹ and N.A. DIANSKY¹

Abstract—The aim of this paper is twofold : To present an efficient numerical technique for the simulation of the ocean general circulation (OGC) and to apply it to the simulation of the Indian Ocean dynamics with high spatial resolution. To solve model equations we use the splitting method by physical processes and space coordinates. We select the main parts of the model operator and then perform their numerical treatment independently of one another. We describe the general methodology and some special aspects of this approach. Numerical treatment of the monsoon circulation is performed on the basis of the sigma-coordinate primitive equation model, which was developed at the Institute of Numerical Mathematics (Moscow, Russia). We present and briefly analyze the results of the numerical experiment with high spatial resolution $1/8^\circ$ along latitude, $1/12^\circ$ along longitude, and with 21 vertical sigma levels.

Key words: Ocean dynamics, monsoon circulation, numerical methods, sigma coordinate, splitting technique.

1. Introduction

The monsoon atmosphere circulation is a key process of the natural environment in the Indo-Asian region (SINGH *et al.*, 1990; SHUKLA and PAOLINO, 1983). The peculiarities of the monsoon circulation affect all aspects of life in the countries situated on the coast of the Indian Ocean. The monsoon precipitation regime above India, the time at which the rainy season begins, rainfall intensity, and the duration of precipitation are the main indicators of the forecast which are necessary for agriculture and industry of India (RAJEEVAN, 2003).

A great amount of heat and moisture, which enters the atmosphere from the surface of the Indian Ocean, defines the peculiarities of the summer southwest monsoon (SINGH *et al.*, 1983). The circulation of the Indian Ocean redistributes heat in the upper ocean layer and consumes the wind energy of the atmosphere and

The work was supported by the Russian Foundation for the Basic Research (03-05-64354, 02-05-64909) and by the Russian Academy of Sciences (10002-251/OMN-03/026-020/240603-807).

¹Institute of Numerical Mathematics RAS, Moscow, Russia

therefore it is of vital importance in the formation and maintenance of the monsoon regime.

To know the structure and the variability of such characteristics of the ocean as sea-surface temperature, heat storage in the upper mixed layer, and currents is necessary for predicting the monsoon circulation. The adequate simulation of the interaction of the atmosphere and the Indian Ocean calls for the development of the system of oceanic observational data assimilation (BARNIER *et al.*, 1994; WENZEL *et al.*, 2001), in the on-line operation as well. When solving the above problem it is impossible to do without modern hydrodynamical models of the circulation of the Indian Ocean.

The aim of the present work is to develop efficient numerical methods of predicting the ocean dynamics. These methods are used for calculating the monsoon circulation in the Indian Ocean, which is characterized by the unique seasonable cycle and complex spatial and temporal variability (SHANKAR *et al.*, 2002). A dramatic peculiarity of the north Indian Ocean is that its currents are radically changed under the action of variable winds of summer and winter monsoons. The observational data show that most currents in the north Indian Ocean reverse their direction from winter to summer (SHANKAR *et al.*, 2002). For the adequate simulation of the complex dynamics of the Indian Ocean and the peculiarities of its eddy structure it is necessary to use models with high spatial resolution, which are physically complete and numerically efficient. We dwell on two aspects of numerical simulation of the ocean dynamics. These are the development of an efficient numerical technique and its application to the simulation of the complex dynamics of the Indian Ocean with high spatial resolution.

OGC models are extremely complex, developing systems. They are based on nonlinear differential equations describing the evolution of three-dimensional velocity, temperature, salinity fields as well as pressure and density. Two main parts can be singled out in the operator of the system of ocean dynamics equations. The first one is the classical established basis, viz. a subsystem describing the dynamics of rotating fluid in the framework of approximations traditional in oceanology (BRYAN, 1969; GILL, 1982; MARCHUK and SARKISYAN, 1988). The second one includes physical parameterizations of various kinds, which change as we gain a better understanding of natural phenomena (GRIFFIES *et al.*, 2000). On this basis we use the decomposition of the problem operator i.e., the splitting method by physical processes as a building block to construct the model and develop efficient numerical methods for solving it. On physical grounds we select the main parts of the operator and then perform their numerical treatment independently of one another. Here we present this line of investigation. We give considerable attention to the description of general methodology of the model construction and the methods of solving the classical part of the OGC equations, we do not dwell on subgrid parameterization. The approach proposed is applied to the solution of the problem of the dynamics of the Indian Ocean. We present

and briefly analyze the results of the numerical simulation of the seasonal cycle of the Indian Ocean circulation with high spatial resolution $1/8^\circ$ along latitude, $1/12^\circ$ along longitude, and with 21 vertical levels.

Numerical treatment of the monsoon circulation is performed on the basis of one version of the model of ocean dynamics, which was developed at the Institute of Numerical Mathematics (ZALESNY, 1996; DIANSKY *et al.*, 2002). The model is based on primitive equations in the Boussinesq, hydrostatics, and “rigid lid” approximations, which are written at the bottom following the σ -coordinate system. In the model the horizontal components of the velocity vector, potential temperature, and salinity are prognostic variables, while the vertical velocity and pressure are diagnostic ones.

The main peculiarity of the model, which distinguishes it from the other ocean models (see the review by GRIFFIES *et al.*, 2000), is that the numerical technique is based on the splitting method by physical processes and space coordinates (MARCHUK, 1980, 1988). To this end, ocean model equations are written in special symmetrized form. The form of the equations is chosen so that it is convenient to represent the operator of the differential problem as a sum of simpler operators, each being nonnegative in the norm defined by the law of conservation of total energy. This enables one to split the operator of the complete problem into a set of simpler operators and construct spatial approximations of the corresponding groups of terms (in different equations) so that the “energy” relation (the conservation law) which holds for the original differential problem should hold for all the splitted discrete problems.

Splitting of model equations is performed at several levels. The macro-level of splitting is splitting of three-dimensional equations by physical processes. At higher levels the process of splitting selects the simplest locally one-dimensional (with respect to the space) equations. For example, the transport-diffusion equation for the tracer is solved along separate coordinates.

The outline of this paper is as follows. In Section 2 we discuss the key features of our approach to the construction and implementation of the OGC model, which is based on the splitting method. The essence of the method is illustrated by simple examples. In Section 3 we formulate the OGC equations, describe the architecture of the splitted model, transformations of the equations at separate splitting stages: their symmetrization and regularization. Particular emphasis is placed upon the choice of the special symmetrized form of ocean dynamics equations in the σ -coordinate system. We provide the form of equations, which allows one to diminish the error of approximation of horizontal pressure gradients on the given profile of vertical density stratification. In Section 4 we discuss the performance and results of the numerical experiment on simulation of the monsoon circulation in the north Indian Ocean with high spatial resolution $1/8^\circ \times 1/12^\circ \times 21$ (steps along latitude, longitude, and the number of σ -levels along the vertical, respectively). In Section 5 we formulate the main conclusions.

2. The Splitting Method as a Methodological Basis for the Construction of a Numerical Model of a Complicated Physical Process

The key points of the approach proposed are as follows.

- The methodological basis for the construction of numerical models of different complexity levels is the splitting method.
- The splitting method can be considered not only as a cost-effective method of integrating the complex OGC problem with respect to the time but as the basis for the construction of the hierarchical model system as well.
- In the framework of the unified approach there can be constructed a particular model of ocean dynamics of a different complexity: from the point of view of its physical completeness, dimension, and spatial resolution.
- The splitting method is defined for solving systems of equations with nonnegative operators. This property is established *a priori* for the differential problem considered. We find an integral invariant or a conservation law which holds in the model in the absence of external sources and internal energy sinks.
- When using the splitting method the form of a differential problem is of great importance. The most convenient form of equations is their symmetrized form. By the symmetrized form we mean the form of equations, which satisfies the conditions:
 - the symmetrized form gives the form of the adjoint operator, which is close to the original one,
 - this form leads to the finite difference approximation retaining the main properties typical of original differential operators (symmetry, skew-symmetry, nonnegativeness),
 - from the form naturally follows the splitting of the problem operator into the sum of simple nonnegative operators.
- The key point of the construction of a splitted hierarchical model system and the method of its solution is the decomposition of the original problem into the set of simple subproblems with nonnegative operators.

The choice of this splitting is frequently nontrivial and not unique (MARCHUK *et al.*, 1987). The splitting process reduces to the choice of a set of separate problems of simpler structure. The established conservation law holds for every selected problem. Several levels of different depth can be selected in splitting. The splitting macro-level is based on splitting by physical processes. The simplest one-dimensional (with respect to space) problems can be selected at higher levels.

- On splitting the problem at a macro-level the transformation of the problem at some stage can be required. This can be, for example, *filtration* (simplification) of equations and *regularization* i.e., the inclusion of additional terms which can improve the numerical algorithm.

- Software and algorithms for solving splitted problems.

On regularizing the splitting stages the question of the choice of a method for solving the problem at the selected stage arises. When choosing a space-approximation technique the property of the selected problem should be taken into account. Different problems (at some stages) can call for different approximation techniques and solvers. In general, the joint model can combine finite-difference schemes and finite-element ones; some problems can be approximated with a higher order of accuracy and so on.

- Module principle and the model software.

The natural property of the splitted model is its module principle: a separate problem — a separate module. The joint model can be “composed” of the different number of modules. The computational characteristics of the model can be improved by changing separate computational modules. Mathematical aspects of the splitting method and its application to the solution of a wide class of physical problems are presented in SAMARSKII (1962), YANENKO (1967), and MARCHUK, (1980, 1988).

The essence of the method is the following. Suppose there is the nonstationary problem

$$\begin{aligned} \frac{\partial \varphi}{\partial t} + A\varphi &= f, & t \in (0, T], \\ \varphi &= \varphi^0 & t = 0 \end{aligned} \quad (2.1)$$

where A is a nonnegative operator which can be represented as superposition of simpler operators $A_i (i = 1, 2, 3, \dots, I)$:

$$A = \sum_{i=1}^I A_i \quad A_i \geq 0, \forall i.$$

To solve (2.1) we use the following method. We reduce the solution of the original problem with the complex operator A to the solution of a set of problems with simpler operators A_i . For example, if $A = A_1 + A_2$, we can use the following two-cycle splitting scheme (MARCHUK, 1988; MARCHUK and SARKISYAN, 1988) to solve the problem (2.1):

$$\begin{aligned} \left(E + \frac{\tau}{2}A_1\right)\varphi^{j-1/2} &= \left(E - \frac{\tau}{2}A_1\right)\varphi^{j-1}, \\ \left(E + \frac{\tau}{2}A_2\right)\varphi^j &= \left(E - \frac{\tau}{2}A_2\right)\varphi^{j-1/2}, \\ \bar{\varphi} &= \varphi^j + 2\tau f^j, \\ \left(E + \frac{\tau}{2}A_2\right)\varphi^{j+1/2} &= \left(E - \frac{\tau}{2}A_2\right)\bar{\varphi}, \\ \left(E + \frac{\tau}{2}A_1\right)\varphi^{j+1} &= \left(E - \frac{\tau}{2}A_1\right)\varphi^{j+1/2}, \quad j = 1, 2, \dots, J-1, \quad \varphi^0 = \varphi(t=0), \quad \tau = T/J. \end{aligned} \quad (2.2)$$

The scheme (2.2) is absolutely stable and approximates (2.1) with the second order of accuracy with respect to time, provided $\frac{\tau}{2} \|A_i\| < 1$.

To solve (2.1) we can also use the simple implicit splitting scheme:

$$\begin{aligned}\bar{\varphi} &= \varphi^j + \tau f^j, \\ (E + \tau A_1) \varphi^{j+1/2} &= \bar{\varphi}, \\ (E + \tau A_2) \varphi^{j+1} &= \varphi^{j+1/2}.\end{aligned}\tag{2.3}$$

The scheme (2.3) is absolutely stable and approximates (2.1) with the first order of accuracy with respect to time. It is more cost-effective than (2.2) but less accurate with respect to time.

The splitting method can be used more widely; on its basis we can develop a numerical model of a complicated process. We can improve the original model by including additional splitting stages into (2.2) or (2.3). We can change the original model. For example, on splitting the problem into a chain of subproblems we can change (simplify and/or regularize) the problem at some stage.

We present a simple example. Assume that when solving some problem we use the procedure of filtering out high-frequency harmonics along the x -coordinate from the solution. To this end, at each time step j we recalculate the vector solution φ^j by the formula

$$\bar{\varphi}_i = (\varphi_{i+1}^j + 2\varphi_i^j + \varphi_{i-1}^j)/4.$$

Writing this formula as

$$(\bar{\varphi}_i - \varphi_i^j)/\tau = \frac{h^2}{4\tau} (\varphi_{i+1}^j - 2\varphi_i^j + \varphi_{i-1}^j)/h^2,$$

we see that the filtering procedure can be considered as the inclusion of an additional splitting stage. At the additional stage we solve the diffusion equation by the explicit scheme:

$$\frac{\partial \varphi}{\partial t} = \mu^\tau \varphi_{xx},$$

where μ^τ is the coefficient of computational viscosity:

$$\mu^\tau = \frac{h^2}{4\tau}.$$

It is not difficult to show that if there is viscosity with the coefficient no less than μ^τ at one of the splitting stages implemented implicitly, then the numerical scheme is absolutely stable.

3. Mathematical Model of Ocean Dynamics

We present the mathematical formulation of the ocean dynamics problem. In the spherical coordinates (λ, θ, z) we have (BRYAN, 1969; ZALESNY, 1996)

$$\begin{aligned}
 \frac{du}{dt} - (l - m \cdot \cos \theta \cdot u)v &= -\frac{m}{\rho_0} \frac{\partial p}{\partial \lambda} + \frac{\partial}{\partial z} v_u \frac{\partial u}{\partial z} + F^u, \\
 \frac{dv}{dt} + (l - m \cdot \cos \theta \cdot u)u &= -\frac{n}{\rho_0} \frac{\partial p}{\partial \theta} + \frac{\partial}{\partial z} v_v \frac{\partial v}{\partial z} + F^v, \\
 \frac{\partial p}{\partial z} &= g\rho_w, \\
 m \left[\frac{\partial u}{\partial \lambda} + \frac{\partial}{\partial \theta} \left(\frac{n}{m} v \right) \right] + \frac{\partial w}{\partial z} &= 0, \\
 \frac{dT}{dt} &= \frac{\partial}{\partial z} v_T \frac{\partial T}{\partial z} + F^T, \\
 \frac{dS}{dt} &= \frac{\partial}{\partial z} v_S \frac{\partial S}{\partial z} + F^S, \\
 \rho_w &= \rho_w(T, S, p), \quad \text{in } D(\lambda, \theta, z)
 \end{aligned} \tag{3.1}$$

where

$$\begin{aligned}
 \frac{d}{dt} &= \frac{\partial}{\partial t} + mu \frac{\partial}{\partial \lambda} + nv \frac{\partial}{\partial \theta} + w \frac{\partial}{\partial z}, \\
 F^* &= m^2 \frac{\partial}{\partial \lambda} \mu_* \frac{\partial^*}{\partial \lambda} + mn \frac{\partial}{\partial \theta} \mu_* \frac{n}{m} \frac{\partial^*}{\partial \theta}.
 \end{aligned}$$

The system of equations (3.1) is considered on the time interval $(0, t]$ in the three-dimensional domain D . The domain D is bounded by the boundary ∂D which consists of the undisturbed sea surface $z = 0$, the lateral (coastal) surface Σ , and the bottom relief $H(\lambda, \theta)$.

The corresponding boundary and initial conditions are added to the above system of equations. In particular, along the vertical coordinate we have for $z = 0$:

$$\begin{aligned}
 v_u \frac{\partial u}{\partial z} &= -\frac{\tau_1}{\rho_0}, \quad v_v \frac{\partial v}{\partial z} = -\frac{\tau_2}{\rho_0}, \quad w = 0, \\
 v_T \frac{\partial T}{\partial z} &= D_T(T_S - T) + Q_T, \quad v_S \frac{\partial S}{\partial z} = D_S(S_0 - S) + Q_S,
 \end{aligned} \tag{3.2}$$

for $z = H(\lambda, \theta)$:

$$w = m \frac{\partial H}{\partial \lambda} u + n \frac{\partial H}{\partial \theta} v. \tag{3.3}$$

On the lateral surface Σ we give the no-slip condition and the conditions of no heat and salt fluxes at the bottom and on Σ .

We give initial conditions for $t = 0$:

$$u = u^0, \quad v = v^0, \quad T = T^0, \quad S = S^0. \quad (3.4)$$

Here λ is the longitude, $\theta = 90 + \psi$, where ψ is the latitude, z is the vertical downward coordinate, (u, v, w) is the velocity field, T is potential temperature, S is salinity, p is pressure, ρ_w is seawater density which is the known function of potential temperature, salinity, and pressure; the terms F^u, \dots, F^S describe the horizontal turbulent transport; v_u, v_v, v_T, v_S are the coefficients of vertical turbulent diffusivity; $\mu_u, \mu_v, \mu_T, \mu_S$ are the corresponding coefficients of horizontal diffusivity, l is the Coriolis parameter: $l = -2\Omega \cos \theta$, $m = \frac{1}{r \sin \theta}$, $n = \frac{1}{r}$, r is the radius of the earth.

The procedure of constructing the numerical model and the algorithm for its numerical treatment includes several successive steps (ZALESNY, 1996). We outline the procedure.

3.1 The Ocean Dynamics Equation in the σ -coordinate System

The first step of the transformations consists in introducing the σ -coordinate system. The σ -transformation introduced into atmospheric models by Phillips more than 40 years ago (PHILLIPS, 1957) has found wide application in solving the problems of meteorology and oceanology (WASHINGTON and PARKINSON, 1986; SINGH *et al.*, 1995; HAIDVOGEL and BECKMANN, 1999). Using this approach, we rewrite (3.1)–(3.3) in the new system $(\lambda_1, \theta_1, \sigma)$: $\lambda_1 = \lambda$, $\theta_1 = \theta$, $\sigma = z/H(\lambda, \theta)$.

In this case we have

$$\frac{\partial}{\partial \lambda} = \frac{\partial}{\partial \lambda_1} - \frac{1}{H} \frac{\partial H}{\partial \lambda_1} \frac{\partial}{\partial \sigma}, \quad \frac{\partial}{\partial \theta} = \frac{\partial}{\partial \theta_1} - \frac{1}{H} \frac{\partial H}{\partial \theta_1} \frac{\partial}{\partial \sigma}, \quad \frac{\partial}{\partial z} = \frac{1}{H} \frac{\partial}{\partial \sigma}.$$

The operators of turbulent transport and boundary conditions are written accordingly.

In the σ -system the continuity equation takes the form

$$m \left[\frac{\partial H u}{\partial \lambda_1} + \frac{\partial}{\partial \theta_1} \left(\frac{n}{m} H v \right) \right] + \frac{\partial w_1}{\partial \sigma} = 0, \quad (3.5)$$

where w_1 is the new vertical velocity

$$w_1 = w - m\sigma \left[\frac{\partial H}{\partial \lambda_1} u + \frac{n}{m} \frac{\partial H}{\partial \theta_1} v \right]. \quad (3.6)$$

The boundary condition for the new vertical velocity at the bottom, for $\sigma = 1$, is the same as at the surface:

$$w_1 = 0. \quad (3.7)$$

3.2 The Total Energy Conservation Law and Macro-splitting of the Problem

We write the hydrostatic equation as

$$\frac{\partial p}{\partial z} = g(\rho + \delta\rho), \quad (3.8)$$

$$\delta\rho = \rho_w - \rho,$$

where ρ is potential density. Unlike the density ρ_w , it does not depend on pressure. If all the terms describing turbulent transport processes are neglected as well as the last term $\delta\rho$ in (3.8), the total energy conservation law holds:

$$\frac{\partial}{\partial t} \int_D \left[H\rho_0 \frac{u^2 + v^2}{2} - \sigma g H^2 \rho \right] dD = 0. \quad (3.9)$$

The second step of the transformations consists in splitting the system of equations (3.1)–(3.3) by physical processes. Allowing for the conservation law (3.9), we single out three energy-independent splitting stages.

As the first subsystem we select equations describing the transport diffusion of momentum, taking into account metric terms. Dropping the subscripts on the variables λ_1, θ_1 , we have

$$\begin{aligned} \frac{du}{dt} + m \cdot \cos \theta \cdot u \cdot v &= \frac{1}{H^2} \frac{\partial}{\partial \sigma} v_u \frac{\partial u}{\partial \sigma} + F_1^u, \\ \frac{dv}{dt} - m \cdot \cos \theta \cdot u \cdot u &= \frac{1}{H^2} \frac{\partial}{\partial \sigma} v_v \frac{\partial v}{\partial \sigma} + F_1^v. \end{aligned} \quad (3.10)$$

As the second subsystem we select the equation of turbulent heat and salt exchange. We have

$$\begin{aligned} \frac{\partial T}{\partial t} &= \frac{1}{H^2} \frac{\partial}{\partial \sigma} v_T \frac{\partial T}{\partial \sigma} + F_1^T, \\ \frac{\partial S}{\partial t} &= \frac{1}{H^2} \frac{\partial}{\partial \sigma} v_S \frac{\partial S}{\partial \sigma} + F_1^S. \end{aligned} \quad (3.11)$$

In (3.10), (3.11) F_l^* are the terms describing the turbulent exchange in the σ -coordinate system. At the third stage we have equations of adjustment of velocity and density fields. We consider this stage in greater detail below.

3.3 Symmetrization of Systems of Equations

The next step of the transformations consists in symmetrizing the obtained systems of equations.

We present a simple example of symmetrization of the transport equation for the tracer φ in the nondivergent flow field. Three forms of the transport equation are known: conventional, divergent, and semidivergent. Using the semidivergent form, we have

$$\frac{H}{m} \frac{\partial \varphi}{\partial t} + \frac{1}{2} \left[Hu \frac{\partial \varphi}{\partial \lambda} + \frac{\partial}{\partial \lambda} (Hu\varphi) + \frac{n}{m} Hv \frac{\partial \varphi}{\partial \theta} + \frac{\partial}{\partial \theta} \left(\frac{n}{m} Hv\varphi \right) + \frac{w_1}{m} \frac{\partial \varphi}{\partial \sigma} + \frac{\partial}{\partial \sigma} \left(\frac{w_1}{m} \varphi \right) \right] = 0. \quad (3.12)$$

From a computational standpoint, the semidivergent form (3.12) has the following useful properties:

- this form admits simple finite-difference approximation retaining the skew-symmetry property (MARCHUK, 1980),
- using this form, it is easy to obtain the decomposition of the operator of the problem into the sum of three simple nonnegative transport operators along the coordinates λ, θ, σ ,
- the operator of the adjoint equation coincides with the original one.

This raises up the question: In what form is it convenient to write the equations at the stage of adjustment of velocity and potential density fields? With the above example in mind, we discuss this question in more detail.

3.4 Symmetrization of Equations of Adjustment of Velocity and Density Fields

Neglecting $\delta\rho$ in the hydrostatic equation for simplicity, at the adjustment stage we have

$$\begin{aligned} \frac{\partial u}{\partial t} - lv + \frac{m}{\rho_0} \left[\frac{\partial p}{\partial \lambda} - \underbrace{g \frac{\partial H\sigma}{\partial \lambda}}_1 \rho \right] &= 0, \\ \frac{\partial v}{\partial t} + lu + \frac{n}{\rho_0} \left[\frac{\partial p}{\partial \theta} - \underbrace{g \frac{\partial H\sigma}{\partial \theta}}_2 \rho \right] &= 0, \\ \frac{1}{\rho_0} \left[\frac{\partial p}{\partial \sigma} - \underbrace{g \frac{\partial H\sigma}{\partial \sigma}}_3 \rho \right] &= 0, \\ m \left[\frac{\partial Hu}{\partial \lambda} + \frac{\partial}{\partial \theta} \left(\frac{n}{m} Hv \right) \right] + \frac{\partial w_1}{\partial \sigma} &= 0, \\ \frac{H}{m} \frac{\partial \rho}{\partial t} + \underbrace{\frac{\partial}{\partial \lambda} (Hu\rho)}_1 + \underbrace{\frac{\partial}{\partial \theta} \left(\frac{n}{m} Hv\rho \right)}_2 + \underbrace{\frac{\partial}{\partial \sigma} \left(\frac{w_1}{m} \rho \right)}_3 &= 0 \end{aligned} \quad (3.13)$$

The adjustment equations (3.13) are written in terms of potential density. This can be done if we assume that potential density is a sufficiently smooth function of potential temperature and salinity.

To the system of equations (3.13) are added the corresponding no-normal flow conditions on the lateral boundary dD as well as the kinematical condition along the vertical:

$$w_1 = 0 \quad \text{for} \quad \sigma = 0, \sigma = 1. \tag{3.14}$$

If we take the inner product of the system (3.13) and the vector

$$(\rho_0Hu, \rho_0Hv, \rho_0w_1, p, -gH\sigma),$$

then with allowance for the boundary conditions the law of conservation of total energy (3.9) holds. It should be noted that the form of the terms depending on density in the first three equations of (3.13) is consistent with the divergent form of the equation for potential density. The terms marked by identical numbers are in pairs energetically neutral.

There exist several different forms of adjustment equations (3.13), which are due to different representations of the terms depending on potential density.

Now we write the equations in more general form. Assume $f = f(\sigma H)$ is some known smooth function of the vertical coordinate $z \equiv \sigma H$ and $f' \equiv \frac{df}{d(\sigma H)} \neq 0$ is its derivative. We write the adjustment equations as

$$\begin{aligned} \frac{\partial u}{\partial t} - lv + \frac{m}{\rho_0} \frac{\partial \tilde{p}}{\partial \lambda} &= \frac{mg}{2\rho_0} \left[\frac{\rho}{f'} \frac{\partial f}{\partial \lambda} - f \frac{\partial}{\partial \lambda} \left(\frac{\rho}{f'} \right) \right], \\ \frac{\partial v}{\partial t} - lu + \frac{n}{\rho_0} \frac{\partial \tilde{p}}{\partial \theta} &= \frac{ng}{2\rho_0} \left[\frac{\rho}{f'} \frac{\partial f}{\partial \theta} - f \frac{\partial}{\partial \theta} \left(\frac{\rho}{f'} \right) \right], \\ \frac{1}{\rho_0} \frac{\partial \tilde{p}}{\partial \sigma} &= \frac{g}{2\rho_0} \left[\frac{\rho}{f'} \frac{\partial f}{\partial \sigma} - f \frac{\partial}{\partial \sigma} \left(\frac{\rho}{f'} \right) \right], \\ m \left[\frac{\partial Hu}{\partial \lambda} + \frac{\partial}{\partial \theta} \left(\frac{n}{m} H v \right) \right] + \frac{\partial w_1}{\partial \sigma} &= 0, \end{aligned} \tag{3.15}$$

$$\begin{aligned} \frac{H}{m} \frac{\partial}{\partial t} \left(\frac{\rho}{f'} \right) + \frac{1}{2} \left[Hu \frac{\partial}{\partial \lambda} \left(\frac{\rho}{f'} \right) + \frac{\partial}{\partial \lambda} \left(Hu \frac{\rho}{f'} \right) + \frac{n}{m} H v \frac{\partial}{\partial \theta} \left(\frac{\rho}{f'} \right) + \frac{\partial}{\partial \theta} \left(\frac{n}{m} H v \frac{\rho}{f'} \right) \right. \\ \left. + \frac{w_1}{m} \frac{\partial}{\partial \sigma} \left(\frac{\rho}{f'} \right) + \frac{\partial}{\partial \sigma} \left(\frac{w_1 \rho}{m f'} \right) \right] = \frac{\rho}{f} \left[Hu \frac{\partial}{\partial \lambda} \left(\frac{f}{f'} - \sigma H \right) \right. \\ \left. + \frac{n}{m} H v \frac{\partial}{\partial \theta} \left(\frac{f}{f'} - \sigma H \right) + \frac{w_1}{m} \frac{\partial}{\partial \sigma} \left(\frac{f}{f'} - \sigma H \right) \right] \end{aligned}$$

where

$$\tilde{p} = p - \frac{g}{2} \frac{\rho}{f'} f.$$

Choosing the form of the function f , we can obtain different forms of model equations.

One of the difficulties in using σ -models of ocean dynamics is associated with the presence of the truncation error of horizontal pressure gradients

(WASHINGTON and PARKINSON, 1986; GRIFFIES *et al.*, 2000). In our case, these are the right-hand sides of the first three equations (3.15) (the terms depending on potential density).

In the geopotential z -system, if density does not depend on the horizontal coordinates λ and θ , motion does not occur. In the σ -system, due to the approximation error of pressure gradients along the surface $\sigma = \text{const}$ nonzero velocities occur. With pronounced density stratification along the vertical and with large gradients of the bottom relief, these fictitious velocities can be significant. Choosing the function f in the special way, we can reduce this effect.

As an illustration we give the following examples. Let potential density depend only on the vertical coordinate $z \equiv \sigma H$ and satisfy

$$\rho = \sigma H.$$

It is easily seen that if we choose f also as

$$f = \sigma H,$$

the right-hand side of the first three equations (3.15) vanishes. It means that the horizontal pressure gradients do not generate in σ -coordinate system artificial velocities.

Assume now that potential density satisfies the condition

$$\rho = \rho_0 e^{z\sigma H}.$$

In this case, we can eliminate errors in the pressure gradients choosing f as

$$f^2 = \rho_0 e^{z\sigma H}.$$

Finally, presume that potential density is an arbitrary function $\tilde{\rho}(\sigma H)$ or it can be approximated by this function with high accuracy. Then choosing the function f as

$$f^2 = 2 \int \tilde{\rho}(\sigma H) d(\sigma H),$$

we can see that for $\rho = \tilde{\rho}(\sigma H)$ the terms in the right-hand sides of (3.15) vanish. Note that with usual finite-difference approximation of the equation of motion this property is satisfied using the staggered grid C in the spatial variables λ, θ, σ .

3.5 Splitting of Adjustment Equations

The adjustment stage is the most tedious stage of calculations. To increase the computational efficiency at this stage we can use further splitting of equations. We demonstrate the splitting procedure at the adjustment stage using, as an example, the symmetrized forms of equations which are consistent with the semidivergent form of the equations for density, i.e., we put $f = \sigma H$ in (3.15).

In this case, at the first internal splitting stage we have

$$\begin{aligned}\frac{\partial u}{\partial t} &= -\frac{mg}{2\rho_0} \left[\sigma H \frac{\partial \rho}{\partial \lambda} - \frac{\partial H \sigma}{\partial \lambda} \rho \right], \\ \frac{\partial v}{\partial t} &= 0, \\ \frac{H}{m} \frac{\partial \rho}{\partial t} + \frac{1}{2} \left[\frac{\partial}{\partial \lambda} (Hu\rho) + Hu \frac{\partial}{\partial \lambda} \rho \right] &= 0.\end{aligned}\tag{3.16}$$

At the second internal splitting stage

$$\begin{aligned}\frac{\partial u}{\partial t} &= 0, \\ \frac{\partial v}{\partial t} &= -\frac{ng}{2\rho_0} \left[\sigma H \frac{\partial \rho}{\partial \theta} - \frac{\partial H \sigma}{\partial \theta} \rho \right], \\ \frac{H}{m} \frac{\partial \rho}{\partial t} + \frac{1}{2} \left[\frac{\partial}{\partial \theta} \left(\frac{nHv\rho}{m} \right) + \frac{n}{m} Hv \frac{\partial}{\partial \theta} \rho \right] &= 0\end{aligned}\tag{3.17}$$

Finally, at the third stage

$$\begin{aligned}\frac{\partial u}{\partial t} - lv + \frac{m}{\rho_0} \frac{\partial p_1}{\partial \lambda} &= 0, \\ \frac{\partial v}{\partial t} + lv + \frac{n}{\rho_0} \frac{\partial p_1}{\partial \theta} &= 0, \\ \frac{\partial p_1}{\partial \sigma} &= -\frac{g}{2} \left[\sigma H \frac{\partial \rho}{\partial \sigma} - \frac{\partial H \sigma}{\partial \sigma} \rho \right], \\ m \left[\frac{\partial Hu}{\partial \lambda} + \frac{\partial}{\partial \theta} \left(\frac{n}{m} Hv \right) \right] + \frac{\partial w_1}{\partial \sigma} &= 0, \\ \frac{H}{m} \frac{\partial \rho}{\partial t} + \frac{1}{2} \left[\frac{\partial}{\partial \sigma} \left(\frac{w_1}{m} \rho \right) + \frac{w_1}{m} \frac{\partial \rho}{\partial \sigma} \right] &= 0, \\ p_1 &= p - \frac{g}{2} \sigma H \rho.\end{aligned}\tag{3.18}$$

Thus, at the first and second splitting stages we arrive at the solution of locally one-dimensional problems along the coordinates λ and θ , while at the third stage - at the more complex three-dimensional problem.

To equations (3.18) are added the boundary no-normal flow conditions. A peculiarity of the formulation of the initial boundary value problem for (3.18), which is typical of hydrodynamic equations, is that there are no boundary conditions for pressure. This leads to additional difficulties when solving numerically the problem, in particular, when calculating pressure along the vertical. In this case, we can use once again additional splitting involving the selection of the vertical-averaged motion component. To this end we write equations (3.18) in the equivalent form from which the solution algorithm naturally follows. We have

$$\begin{aligned}
 \frac{\partial u}{\partial t} - l(v - \bar{v} + \bar{v}) + \frac{m}{\rho_0} \frac{\partial p'_1}{\partial \lambda} + R\bar{u} &= -\frac{m}{\rho_0} \frac{\partial \bar{p}_1}{\partial \lambda} + R\bar{u}, \\
 \frac{\partial v}{\partial t} + l(u - \bar{u} + \bar{u}) + \frac{n}{\rho_0} \frac{\partial p'_1}{\partial \theta} + R\bar{v} &= -\frac{n}{\rho_0} \frac{\partial \bar{p}_1}{\partial \theta} + R\bar{v}, \\
 \frac{\partial H\bar{u}}{\partial \lambda} + \frac{\partial}{\partial \theta} \left(\frac{n}{m} H\bar{v} \right) &= 0, \\
 m \left[\frac{\partial H(u - \bar{u})}{\partial \lambda} + \frac{\partial}{\partial \theta} \left(\frac{n}{m} H(v - \bar{v}) \right) \right] + \frac{\partial w_1}{\partial \sigma} &= 0, \\
 \frac{H}{m} \frac{\partial \rho}{\partial t} + \frac{1}{2} \left[\frac{\partial}{\partial \sigma} \left(\frac{w_1}{m} \rho \right) + \frac{w_1}{m} \frac{\partial \rho}{\partial \sigma} \right] &= 0,
 \end{aligned}
 \tag{3.19}$$

where

$$\bar{a} = \int_0^1 a \, d\sigma, \quad (a = u, v), \quad \bar{p}_1 = p_1(0) - \frac{g}{2} \int_0^1 d\sigma \int_0^\sigma \left(\sigma H \frac{\partial \rho}{\partial \sigma} - \frac{\partial \sigma H}{\partial \sigma} \rho \right) d\sigma, \quad p'_1 = p_1 - \bar{p}_1,$$

R is some nonnegative function, for example $R = \text{const} \equiv \varepsilon, 0 \leq \varepsilon < 1$.

Using the above representation, we develop the solution algorithm. It consists in solving the following three subsystems. The first subsystem is

$$\begin{aligned}
 \frac{\partial u}{\partial t} &= R\bar{u}, \\
 \frac{\partial v}{\partial t} &= R\bar{v}, \\
 \frac{\partial \rho}{\partial t} &= 0.
 \end{aligned}
 \tag{3.20}$$

The second subsystem is

$$\begin{aligned}
 \frac{\partial u}{\partial t} - l\bar{v} + \frac{m}{\rho_0} \frac{\partial \bar{p}_1}{\partial \lambda} + R\bar{u} &= 0, \\
 \frac{\partial v}{\partial t} + l\bar{u} + \frac{n}{\rho_0} \frac{\partial \bar{p}_1}{\partial \theta} + R\bar{v} &= 0, \\
 \frac{\partial H\bar{u}}{\partial \lambda} + \frac{\partial}{\partial \theta} \left(\frac{n}{m} H\bar{v} \right) &= 0, \\
 \frac{\partial \rho}{\partial t} &= 0.
 \end{aligned}
 \tag{3.21}$$

The third subsystem is

$$\begin{aligned}
 \frac{\partial u}{\partial t} - l(v - \bar{v}) + \frac{m}{\rho_0} \frac{\partial p'_1}{\partial \lambda} &= 0, \\
 \frac{\partial v}{\partial t} + l(u - \bar{u}) + \frac{n}{\rho_0} \frac{\partial p'_1}{\partial \theta} &= 0,
 \end{aligned}
 \tag{3.22}$$

$$\frac{H}{m} \frac{\partial \rho}{\partial t} + \frac{1}{2} \left[\frac{\partial}{\partial \sigma} \left(\frac{w_1}{m} \rho \right) + \frac{w_1}{m} \frac{\partial \rho}{\partial \sigma} \right] = 0,$$

where

$$\frac{w_1}{m} = \int_{\sigma}^0 \left[\frac{\partial H(u - \bar{u})}{\partial \lambda} + \frac{\partial}{\partial \theta} \left(\frac{nH(v - \bar{v})}{m} \right) \right] d\sigma.$$

Note that by selecting depth-averaged motion we obtain the following result. In numerical calculations two boundary conditions along the vertical for the velocity w_1 are exactly satisfied, and correct calculations of the vertical structure of the pressure field are performed.

3.6 Regularization of Problems at Some Splitting Stages

The procedure of ε -regularization is frequently used to increase the stability of the numerical solution. The method of ε -regularization involves the addition of certain terms with small coefficients $\varepsilon < 1$ to the original equation. The method of artificial compressibility, which is proposed by YANENKO (1967) for solving equations of viscous incompressible fluid, can serve as an example of the ε -regularization procedure. The idea of the artificial compressibility method is to replace the continuity equation by a nonstationary equation of the form

$$\varepsilon \frac{\partial p}{\partial t} + \frac{\partial u}{\partial x} + \frac{\partial v}{\partial y} = 0, \quad 0 < \varepsilon < 1.$$

We apply the above approach to regularization of the problem (3.19). We drop the ‘‘rigid lid’’ condition at the undisturbed ocean surface and instead of it we use

$$w = -\frac{1}{g\rho_0} \frac{\partial p_0}{\partial t}, \quad (3.23)$$

where

$$p_0 = -g\rho_0\zeta,$$

ζ – is the ocean surface height.

From a mathematical standpoint, the transition from the model with the ‘‘rigid lid’’ approximation to the ‘milder’ dynamical condition can be considered as regularization of the two-dimensional incompressible fluid dynamics problem. In this case, the efficiency of calculations of the depth-averaged velocities increases.

Physically, the transition to the boundary condition (3.23) implies the introduction of the dynamics of external gravity waves into the model (GILL, 1982; MARCHUK *et al.*, 1987). In this case, in the chain of splitted subsystems, only the stage describing

evolution of the vertical-averaged fields changes. In the terms $\bar{u}, \bar{v}, \bar{p}$ the equations have the form

$$\begin{aligned} \frac{\partial \bar{u}}{\partial t} - l \cdot \bar{v} + \frac{m}{\rho_0} \frac{\partial \bar{p}_1}{\partial \lambda} + R\bar{u} &= 0, \\ \frac{\partial \bar{v}}{\partial t} + l \cdot \bar{u} + \frac{n}{\rho_0} \frac{\partial \bar{p}_1}{\partial \theta} + R\bar{v} &= 0, \\ \frac{1}{g\rho_0} \frac{\partial p_0}{\partial t} + m \left[\frac{\partial H\bar{u}}{\partial \lambda} + \frac{\partial}{\partial \theta} \left(\frac{n}{m} H\bar{v} \right) \right] &= 0, \\ \frac{\partial \rho}{\partial t} &= 0, \\ \bar{p}_1 &= p_0 - \frac{g}{2} \int_0^1 d\sigma \int_0^\sigma \left(\sigma H \frac{\partial \rho}{\partial \sigma} - \frac{\partial \sigma H}{\partial \sigma} \rho \right) d\sigma. \end{aligned} \quad (3.24)$$

To the system (3.24) on the closed coastal boundary Σ are added the no-normal flow conditions.

Note

When writing the third subsystem of equations of adjustment of velocity and potential density fields (3.19) we added and subtracted the terms $Ru, Rv, R \ll 1$. On the one hand, this is an equivalent transformation of the differential system. On the other hand, using the splitting algorithm (3.20)–(3.22) to solve the problem, we can increase the efficiency of calculations of vertical-averaged motion. It is not difficult to show that the splitting scheme is absolutely stable and has the first order of accuracy with respect to time if we use an explicit scheme to solve (3.20) and an implicit one to solve (3.21). If the stage (3.20) is dropped in the hierarchical model system, this can also be considered as ε -regularization of the original problem. In this case, regularization involves the introduction of friction with the coefficient R , which acts on the depth-averaged flow component.

4. The Numerical Experiment on Simulation of Monsoon Circulation in the Indian Ocean

The method presented was used as the basis for constructing the numerical model of monsoon circulation in the Indian Ocean with high spatial resolution.

The computational domain covered the north Indian Ocean (10°S–30°N, 38°E–103°E). The spatial resolution was $1/8^\circ \times 1/12^\circ \times 21$. The bottom topography was interpolated to the computational grid from the five-minute data array ETOPO5. The minimum bottom depth in the domain was 7 m, the maximal one was about 6000 m.

When treating vertical-averaged flows the stage (3.20) was dropped. To solve the equations describing the adjustment of velocity and density fields we put $f = \sigma H$ in (3.15). Horizontal eddy diffusivity was $1.0 \times 10^2 \text{ m}^2/\text{s}$, eddy viscosity was $1.0 \times 10^3 \text{ m}^2/\text{s}$, and the friction coefficients R was $1.0 \times 10^{-6} \text{ s}^{-1}$. Vertical mixing was parameterized using the scheme of PAKANOWSKI and PHILANDER (1981).

The aim of the experiment was to calculate the dynamically consistent seasonable cycle of velocity, temperature, and salinity fields of the Indian Ocean. The model was driven at the sea surface by wind-stress (NCEP reanalysis) and by prescribed temperature and salinity (LEVITUS *et al.*, 1998). The model was spun up for seven years from a state of rest and January temperature and salinity (LEVITUS *et al.*, 1998).

Figures 1–3 present the model instantaneous velocity fields at depths of 60 m, 400 m, and 1000 m. The calculated flows differ widely during the winter and summer monsoons, as the observational data show (TOMCZAK and GODFREY, 2003; SHANKAR *et al.*, 2002).

We shall dwell briefly on the structure and seasonal variability of the main currents in the Indian Ocean and compare them with the observational data.

Equatorial currents. The numerical experiment shows that the North Equatorial Current is observed from January to March when the winter monsoon is fully established. The horizontal velocities are about 0.5–1.0 m/s near the coasts of Sri Lanka, in the sector between the equator and 6°N as well as between 60°E and 75°E. In the equatorial zone the westward Equatorial Counter Current with the velocities of order 0.5–0.8 m/s is observed. The current is located to the south of 2°S, and its intensity is diminished westward. According to the calculations this current does not extend farther than 70°E and merges with the westward countercurrent which is approximately equal in intensity. This pattern is in good agreement with the observational study (TOMCZAK and GODFREY 2003), except that the countercurrent is much weaker according to the data. During the months of the monsoon change the Indian Equatorial Jet with velocities 0.7 m/s and higher is pronounced. In the period of the summer monsoon the model also reproduces the Southwest Monsoon Current (TOMCZAK and GODFREY 2003) which reaches the velocities 0.5–0.8 m/s south and southeast of Sri Lanka.

Currents in the Arabian Sea and the Bay of Bengal. The model describes adequately the structure of the Somali Current as well as the appearance of the Great Whirl towards the end of the summer monsoon. In September the velocities reach 2 m/s at a depth of 30 m. In March and in January the current reverses its direction.

In summer the northeastward and southeastward Summer Monsoon Current (SHANKAR *et al.*, 2002) flows across the Arabian Sea basin (Fig. 1). It divides into two branches off Oman at approximately 15°N. In one branch, which is situated close to the Oman coast, water moves clockwise and forms the West India Coastal Current (WICC) off India (SHANKAR *et al.*, 2002). The second branch deviates from the coastal current into the open ocean and forms the Summer

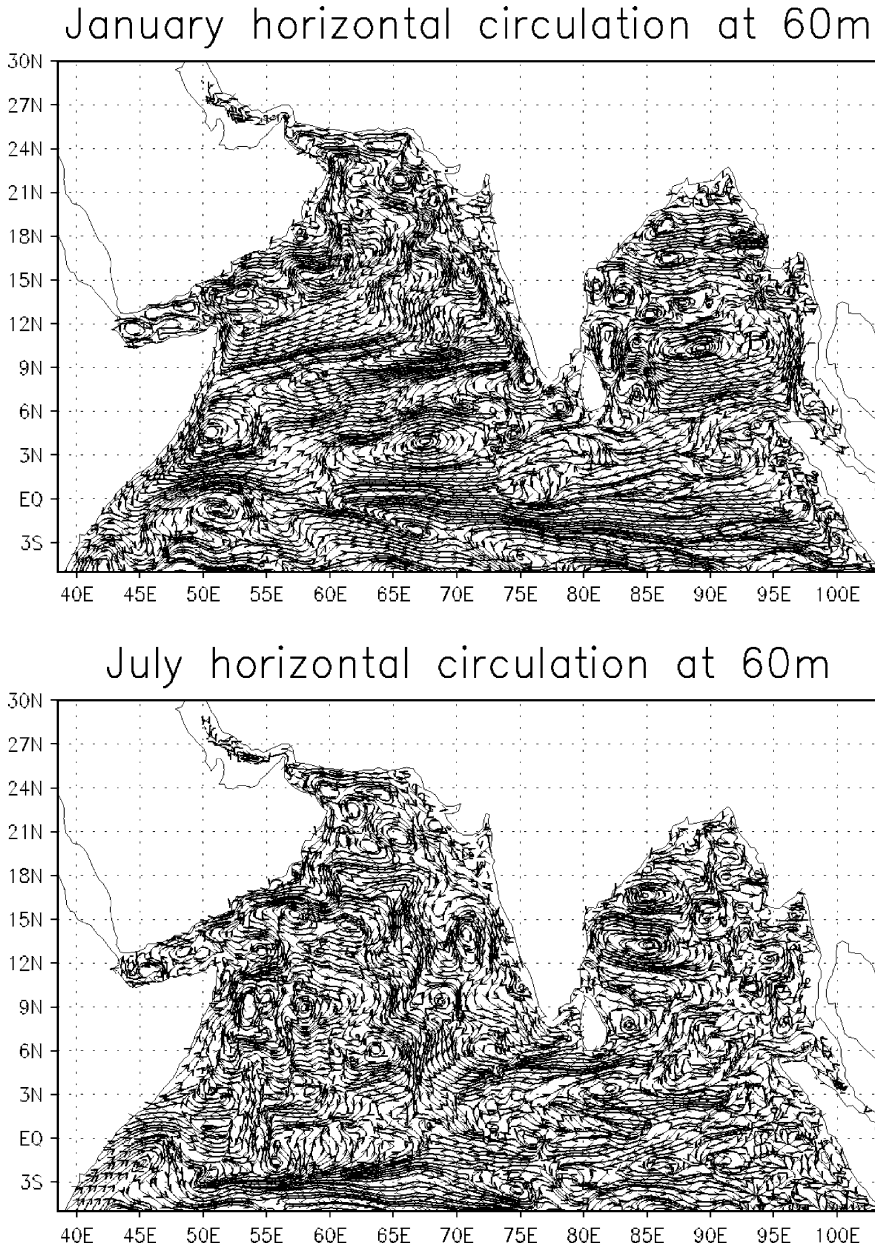


Figure 1
Model instantaneous velocity fields at depth 60 m.

Monsoon Current (SMC) (Shankar *et al.*, 2002). It should be noted that the complete pattern of currents is rather complex. There are several cyclones and anticyclones inside the Arabian Sea, between two main currents. In the period of

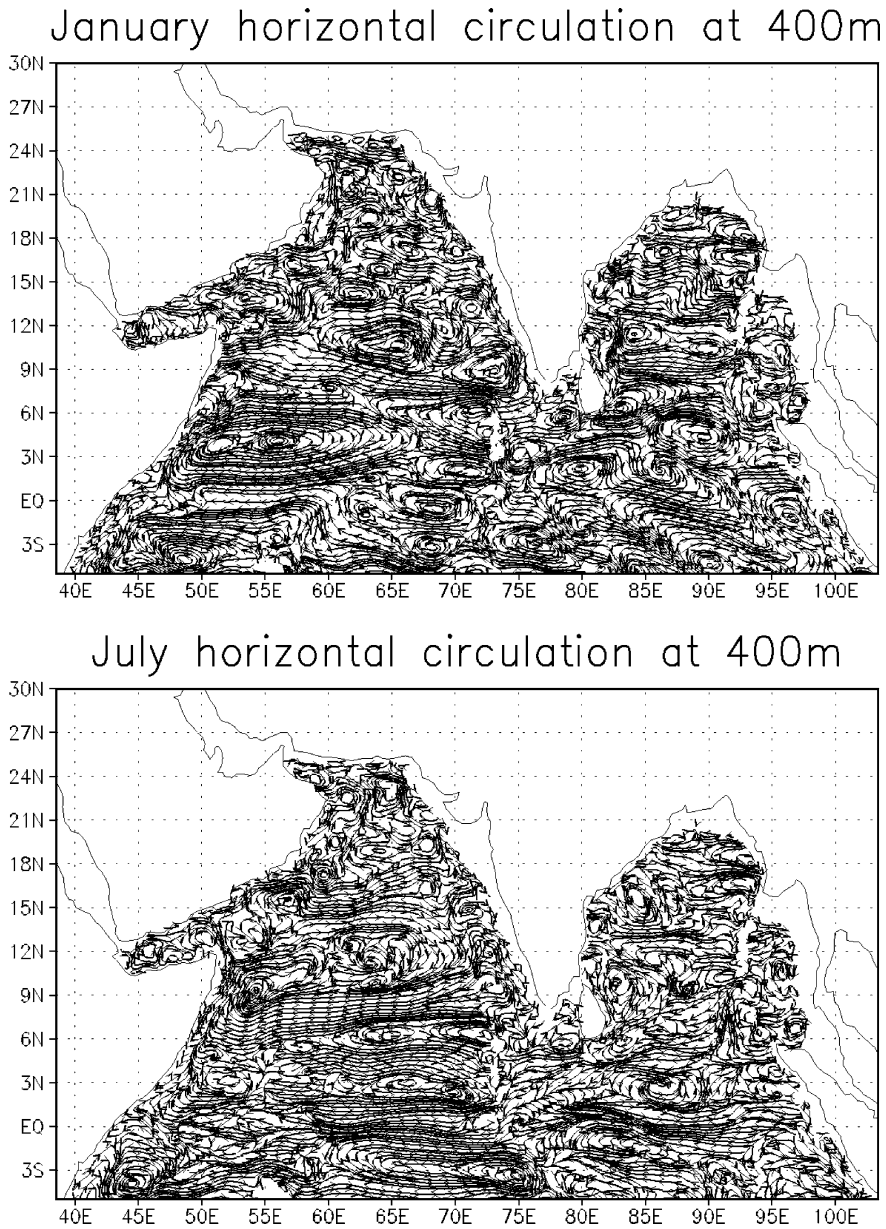


Figure 2
Model instantaneous velocity fields at depth 400 m.

the winter monsoon the structure of the velocity field is also rather complex (Fig. 1). In January the Somali Current reverses its direction. Along the entire western coastline of India there appears the coastal northwestward current in the

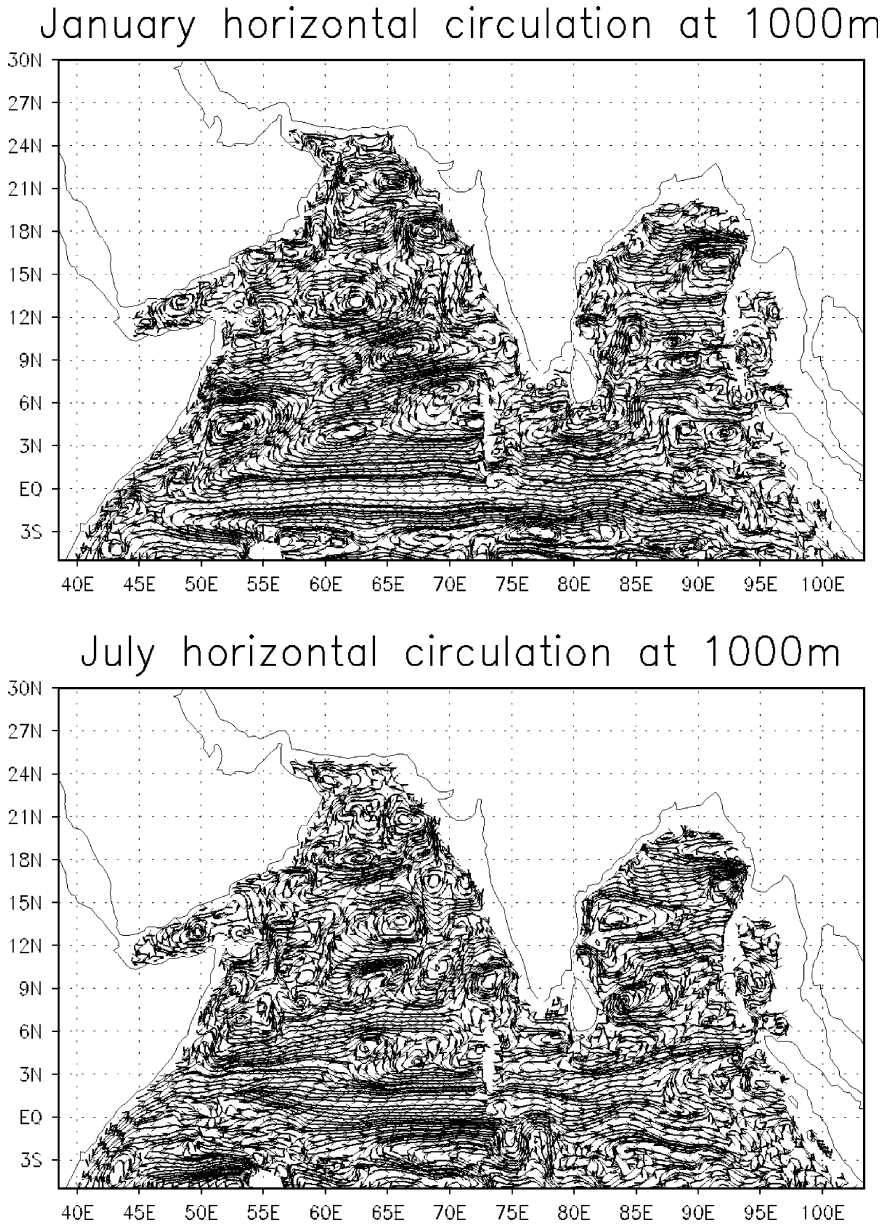


Figure 3
Model instantaneous velocity fields at depth 1000 m

opposite direction as compared to the summer period. Along most of the coastline of the Arabian Sea the currents also reverse their direction as compared to the summer season. There are many local eddies and countercurrents.

The anticyclonic circulation prevails in the Bay of Bengal during most of the year. In March-April the local, rather stable anticyclonic vorticity develops northeast of Sri Lanka. Its horizontal size is about 500 km, its thickness is of order 200 m, the velocities reach 0.8 m/s. By September the eddy intensity is diminished; at the end of October-November the circulation reverses its direction and becomes cyclonic. Several eddies are formed; their total large-scale structure may be interpreted as the East Indian Winter Jet (TOMCZAK and GODFREY 2003). The Jet velocities are of order 0.4–0.7 m/s. The structure of currents is close to the scheme constructed by the observational data (TOMCZAK and GODFREY 2003) though the pattern differs from the scheme by certain details. At 75° – 77° E, south of Sri Lanka, the East Indian Winter Jet meets with the countercurrent entering into the Bay of Bengal. This countercurrent is formed farther west in the open ocean by the eastward current because of its division into two branches. The first branch turns southward and merges with the Equatorial Jet (TOMCZAK and GODFREY 2003). The second one first flows northeastward along the eastern periphery of the above cyclone, flows around it and turns southward forming the countercurrent off Sri Lanka. Water returns into the Arabian Sea, following two paths. First, as the narrow jet about 40 m in depth through the shallow strait between India and Sri Lanka. Second, along the western periphery of the cyclone off the east coast of Sri Lanka as in TOMCZAK and GODFREY (2003).

The vertical structure of currents in the north Indian Ocean is rather complex (Figs. 2 and 3). However, there is one common property: The currents are of distinct zonal character in deeper layers below 300 m. Currents are less intensive and better regulated. The experiment shows that even in the deep ocean the variability of currents with time is appreciable. However, it should be noted that variability is typical of open-ocean eddies rather than the large-scale currents themselves.

5. Conclusion

- In the paper we set forth a common approach to the construction of a numerical model of ocean dynamics which is based on splitting by physical processes and geometric coordinates. Model equations are split on several levels. The splitting macro-level is splitting of three-dimensional equations by physical processes. On higher levels the splitting process is to select the simplest equations which are locally one-dimensional with respect to space. The application of the above approach to the solution of the problem of the Indian Ocean circulation with high spatial resolution demonstrated that this numerical technique performs well.
- The peculiarity of the numerical model of the Indian Ocean dynamics is that the adjustment equations of potential density and velocity fields are written in the sigma-coordinate system in the generalized symmetrized form. This transforma-

tion allows one to decrease truncation errors occurring in horizontal pressure gradient terms in the sigma model and construct a stable computational procedure.

- A comparison of the results of the Indian Ocean simulation with the schemes of currents constructed on the basis of observational data (SHANKAR *et al.*, 2002; TOMCZAK and GODFREY 2003) shows that the model reproduces the monsoon circulation reasonably well. The high resolution enables us to reproduce not only the large-scale structure of monsoon currents, but to describe local peculiarities of its space-time variability as well. The calculations show the high eddy activity of the Indian Ocean. Numerous cyclones and anticyclones are observed in the open ocean, coastal areas, and the deep ocean. Ocean eddies can modify the structure of basin scale currents. With high spatial resolution which is accompanied by the high eddy activity, requirements for the observational data are greater. For the detailed assessment of model calculations and forecasts it is essential to have comprehensive spatial observations. Satellite observations can supply the information regarding the ocean surface; however, to have such information about deep ocean layer is an unresolved problem. The development of observing systems such as the profiling floats ARGO can in part fill the gap. However, in this case, to solve an extremely complex problem of observational data processing and assimilation in the moving coordinate system (of the type of Lagrangian coordinates) is required.

REFERENCES

- BARNIER, B., CAPELLA, J., and O'BRIEN, J.J. (1994), *The Use of Satellite Scatterometer Winds to Drive a Primitive Equation Model of the Indian Ocean: The Impact of Bandlike Sampling*, J. Geophys. Res. 99, C7, 14,187–14,196.
- BRYAN, K. (1969), *A Numerical Method for the Study of the Circulation of the World Ocean*, J. Comput. Physics 4, 347–376.
- DIANSKY, N.A., BAGNO, A. V., and ZALESNY, V. B. (2002), *Sigma Model of Global Ocean Circulation and Its Sensitivity to Variations in Wind Stress*. Izvestiya, Atmospheric and Oceanic Physics (Izvestiya Rossiiskoi Akademii Nauk Fizika Atmosfery i Okeana). 38, No. 4, 477–494.
- GILL, A.E. (Ed.) *Atmosphere-Ocean Dynamics* (Academic Press, New York 1982).
- GRIFFIES, S.M., BOENING C., BRYAN F.O., CHASSIGNET, E.P., GERDES, R., HASUMI, H., HIRST, A., TREGUIER, A.-M., and WEBB, D. (2000), *Developments in Ocean Climate Modelling*, Ocean Modelling 2, 123–192.
- HAIDVOGEL, D.B. and BECKMANN, A., *Numerical Ocean Circulation Modelling* (Imperial College Press, 1999).
- LEVITUS, S., BOYER, T.P., CONKRIGHT, M.E., O'BRIEN, T., ANTONOV, J., STEPHENS, C., STATHOPOLOS, L., JOHNSON, and D., GELFELD R. (1998), NOAA Atlas NESDIS 18, *World Ocean Database 1998*: Vol. 1: Introduction (U.S. Gov. Printing Office, Washington, D.C.) 346 pp.
- MARCHUK, G.I., *Methods of Computational Mathematics* (Nauka, Moscow 1980).
- MARCHUK, G.I., *Splitting-up Methods* (Nauka, Moscow 1988).
- MARCHUK, G.I., DYMNIKOV, V.P., and ZALESNY, V.B., *Mathematical Models in Geophysical Hydrodynamics and Numerical Methods of their Realization* (Gidrometeoizdat, Leningrad 1987).
- MARCHUK, G.I. and SARKISYAN, A.S., *Mathematical Modelling of Ocean Circulation* (Springer-Verlag, Berlin, Heidelberg, New York, London, Paris, Tokyo 1988).

- PHILLIPS, N.A. (1957), *A Coordinate System Having Some Special Advantages for Numerical Forecasting*, J. Meteorology 14, 184–185.
- RAJEEVAN, M. (2003), *Prediction of Indian Summer Monsoon: Status Problems and Prospects*, Curr. Science 11, 1451–1457.
- SAMARSKII, A.A. (1962), *On Convergence of the Fractional-step Method for Heat Equation*, Zh. Vych. Mat. Mat. Fiz. 2, 6, 1117–1121.
- SHANKAR, D., VINAYACHANDRAN, P.N., UNNIKRISHNAN, A.S., and SHETYE, S.R. (2002), *The Monsoon Currents in the North Indian Ocean*, Progr. Oceanogr. 52(1), 63–119.
- SHUKLA, J. and PAOLINO, D.A. (1983), *The Southern Oscillation and Long-range Forecasting of the Summer Monsoon Rainfall in Peninsular India*, Mausam 33, 399–404.
- SINGH, M.P., MOHANTY U.C., and DUBE S.K. (1983), *A Study of Heat and Moisture Budget over the Arabian Sea and their Role in the Onset and Maintenance of Summer Monsoon*, J. Met. Soc. Japan 61, 218.
- SINGH, M.P., RAMAN, S., TEMPLEMAN, B., TEMPLEMAN, S., HOLT T., MURTHY, A.B., AGARWAAL P., NIGAM, S., PRABHU A., and AMEENULLAH S. (1990), *Structure of the Indian Southwesterly Pre-monsoon and Monsoon Boundary Layers: Observations and Numerical Simulation*, Atmosf. Environ. 24A, 723–734.
- SINGH, M.P., SHARAN, M., and YADAV, A.K. (1995), *Comparison of Various Sigma Schemes for Estimating Dispersion of Air Pollutants in Low Winds*, Atmosf. Environ. 29, 2501–2509.
- TOMCZAK, M., and GODFREY, S.J., *Regional Oceanography: An Introduction* (Pergamon 2003).
- WASHINGTON, W.M., and PARKINSON, C.L., *Three-dimensional Climate Modeling* (University Science Books, Mill Valley, California; Oxford University Press, Oxford, New York 1986).
- WENZEL, M., SHROETER, J., and OLBERS, D. (2001), *The Annual Cycle of the Global Ocean Circulation as Determined by 4D VAR Data Assimilation*, Progress in Oceanog. 48, 73–119.
- YANENKO, N.N., *Fractional-step Method of Solving Multidimensional Problems of Mathematical Physics* (Nauka, Novosibirsk 1967).
- ZALESNY, V.B. (1996), *Numerical Simulation and Analysis of the Sensitivity of Large-scale Ocean Dynamics*, Russ. J. Numer. Anal. Math. Modelling 11, 6, 421–443.

(Received September 30, 2003, accepted January 21, 2004)

Published Online First: May 25, 2005



To access this journal online:

<http://www.birkhauser.ch>
